Including strain in atomistic tight-binding Hamiltonians: An application to self-assembled InAs/GaAs and InAs/InP quantum dots

M. Zieliński*
Instytut Fizyki UMK, Grudziądzka 5, 87-100 Toruń, Poland
(Received 6 March 2012; revised manuscript received 20 July 2012; published 17 September 2012)

A method for inclusion of strain into the tight-binding Hamiltonian is presented. This approach bridges from bulk strain to the atomistic language of bond lengths and angles, and features a diagonal parameters shift in a form suitable for atomistic calculation of million atom nanosystems with a small number of empirical parameters. I illustrate this method by calculating electronic and optical properties of self-assembled InAs/(InP,GaAs) lens-shaped quantum dots. A very different structure of confined quantum dots states is shown, depending on the matrix material and inclusion of strain effects. Results are compared with the well-established empirical pseudopotential method, and reasonable agreement is found.

DOI: 10.1103/PhysRevB.86.115424 PACS number(s): 73.21.La, 71.15.−m, 73.22.−f, 71.55.Eq

I. INTRODUCTION

Semiconductor quantum dots (QDs) have gained a significant interest with potential applications in photonics, sensors, quantum information, and cryptography.[1–4] Quantum dot properties such as size, shape, and composition can be tailored and the position can be controlled by growth, e.g., on patterned substrates[5] or by vapor-liquid-solid (VLS) growth in nanopillars.[6,7]

Continuous matter approaches like the effective mass approximation or k*p method proved to be capable of describing main features in the electronic and optical spectrum of QDs.[1,2] Yet these methods are limited by the fact that the resolution on the scale of a unit cell is lost.[3] Proper description of true atomistic symmetry is of paramount importance if both qualitative and quantitative predictions are to be made. One of the most striking examples concerns the bright exciton splitting, which is present even for fully shape-symmetric dots,[8–10] where the straightforward k*p theory predicts no splitting in this case[11,12] and sophisticated multiband k*p approaches are needed to accommodate for the correct symmetry of the underlying crystal lattice.[13–15] Another difference with respect to continuous matter approaches is the hole charging pattern of positively charged exciton complexes in InAs/GaAs lens-shaped self-assembled quantum dots, where the empirical pseudopotential (EPM) method predicts breaking of the Aufbau principle.[16] Clearly theory including atomistic details that accounts for lattice symmetry, material interfaces, and substrate orientation is crucial for understanding optical spectra of quantum dots including exciton fine structure or multiexcitonic properties.

Due to the lattice mismatch of quantum dot and surrounding matrix materials, strain effects must be taken into account as an integral part of any realistic modeling.[17–22] In an atomistic calculation,[23–38] the customary bulk description, that is the language of strain tensor and deformation potentials,[17] needs to be transferred into a microscopic picture of bond lengths and angles.[39] Since strain effects change bond lengths and angles, the Hamiltonian matrix will change accordingly. In the tight-binding (TB) formalism[40] the Hamiltonian matrix elements can be divided into two groups: same-site (diagonal matrix elements) and off-site (off-diagonal) matrix elements, which under nearest neighbors approximation couple orbitals belonging to neighboring atoms only. Strain has been traditionally incorporated by modification of off-diagonal matrix elements only,[40] while leaving the on-site terms unchanged. In work by Jancu *et al.*[41,42] it is argued that on-site diagonal matrix elements might, in principle, also vary due to strain, so strain-induced diagonal correction terms are introduced. The correction is expressed in terms of a microscopic strain tensor which, however, is not unambiguous in an atomistic calculation. To overcome this difficulty Boykin *et al.* introduced a diagonal correction[43,44] expressed in a form more suitable for an atomistic tight-binding approach, yet at a cost of having a complicated model with many empirical parameters. Recently Niquet *et al.*[45] and Boykin *et al.*[46] even further expanded their tight-binding approaches by introducing same site, off-diagonal matrix elements for accurate modeling of uniaxial [111] and [110] strains. These are complex models introducing a substantial number of empirical parameters.

In this work I adopt the well-established Jancu *et al.* model[41] and obtain strain correction to the empirical tight-binding (ETB) Hamiltonian expressed in terms of bond lengths and angles, thus suitable for atomistic calculation, with one (on-site) empirical parameter per material only. I demonstrate the usefulness of my approach by calculating the single particle energy spectra, charge density distributions, and Coulomb integrals of a lens-shaped InAs quantum dot embedded in GaAs and InP matrices. I compare my results with those obtained by the well recognized empirical pseudopotential method (EPM)[28–32] and a different ETB scheme[43,44] and obtain reasonable agreement. I discuss the origins of divergences and find that in an empirical calculation, spectral features at different energy scales can be reproduced at the accuracy appropriate for that scale, depending on a given empirical method and a particular parametrization.

II. STRAIN EFFECTS AND THE ON-SITE CORRECTION

The single-particle tight-binding Hamiltonian for the system of N atoms and m orbitals per atom can be written in the language of the second quantization (in the site basis) in the

following form:

$$\hat{H}_{TB} = \sum_{i=1}^{N}\sum_{\alpha=1}^{m} E_{i\alpha}c_{i\alpha}^{+}c_{i\alpha} + \sum_{i=1}^{N}\sum_{\alpha=1,\beta=1}^{m} \lambda_{i\alpha,\beta}c_{i\alpha}^{+}c_{i\beta} + \sum_{i=1}^{N}\sum_{j=1}^{4}\sum_{\alpha,\beta=1}^{m} t_{i\alpha,j\beta}c_{i\alpha}^{+}c_{j\beta}, \quad (1)$$

where $c_{i\alpha}^{+}$ ($c_{i\alpha}$) is the creation (annihilation) operator of a carrier on the orbital α localized on the site i, $E_{i\alpha}$ is the corresponding on-site (diagonal) energy, and $t_{i\alpha,j\beta}$ describes the hopping (off-site, off-diagonal) of the particle between orbitals on (four) nearest neighboring sites. Coupling to further neighbors is neglected. Finally, $\lambda_{i\alpha,\beta}$ (on-site, off-diagonal) accounts for the spin-orbit interaction following the description given by Chadi.[47]

It was recently found that even for unstrained systems, the inclusion of d-orbitals is necessary for a proper description of conduction states in quantum dots, especially for small size nanocrystals.[33,35] For strained systems, TB models not accounting for d-orbitals (sp^3s^*) yield incorrect signs of indirect gap deformation potentials,[41] therefore realistic, quantitative modeling of nanosystems should incorporate effects of d-orbitals. A more detailed discussion of the $sp^3d^5s^*$ Hamiltonian was given in our previous work.[37,38]

The Slater-Koster[39] approach naturally introduces the strain effects into the model as changes in bond angles are taken into account by the set of rules involving direction cosines $t_{i\alpha,j\beta}$. While to account for changes in bond lengths a generalized version of Harrison law is typically used:[40] $V_{\alpha\beta,\gamma} = V^0_{\alpha\beta,\gamma}(d_{ij}/d_0)^{\eta}$, where $V^0_{\alpha\beta,\gamma}$ is two-center integral for the unstrained case, d_{ij}/d_0 is the ratio of the new to ideal (bulk) bond length, and the exponent η is fitted to reproduce bulk deformation potentials. The modified $V_{\alpha\beta\gamma}$ are used to build tight-binding Hamiltonian matrix elements t_{ij} for the strained system. The above formalism modifies only off-diagonal, off-site (hopping) matrix elements coupling neighboring atoms.

Jancu *et al.*[41] argue that on-site diagonal matrix elements might, in principle, also vary due to strain and introduce uniaxial strain-induced ("crystal field") splitting of otherwise degenerate d levels: E_{xy}, E_{yx}, E_{zx}, which for uniaxial [001] strain are given as

$$\begin{aligned} E_{xy} &= E_d[1 + 2b_d(\epsilon_{zz} - \epsilon_{xx})] \\ E_{xz} &= E_{yz} = E_d[1 - b_d(\epsilon_{zz} - \epsilon_{xx})], \end{aligned} \quad (2)$$

where b_d is the empirical parameter fitted to reproduce uniaxial deformation of the valence band edge, and ϵ_{zz} and ϵ_{xx} are elements[17] of strain tensor ϵ. Biaxial strain introduces asymmetry to the system, acting as effective crystal field, and brakes the degeneracies of orbitals centered along different axis, for example E_{xy} would split from E_{yz} and E_{zx} orbitals under [001] strain or E_{yz} would split form E_{xy} and E_{zx} under [100] strain, etc.

In subsequent work Jancu and Voisin[42] claim that a tight-binding model with d-orbitals requires diagonal matrix element shift to correctly reproduce uniaxial [111] strain for cubic semiconductors and extend their model by additional splitting of atomic p levels. Authors introduce in total three strain related empirical parameters due to the diagonal correction in addition to Harrison law exponents, all fitted to reproduce bulk properties.

In practical terms it is very difficult to get a satisfactory fit to experimental bulk deformation potentials using $sp^3d^5s^*$ TB model without such diagonal corrections. The problem is, however, that the modification of diagonal matrix elements defined in terms of bulk strain tensor elements is not immediately applicable for atomistic calculation. Matrix elements should be defined in terms of quantities dependent on bond lengths and angles, rather then bulk quantities such as strain tensor elements.

Boykin *et al.*[43] argue that tight-binding orbitals are not true atomic orbitals, but rather the orthogonalized Löwdin orbitals. Thus diagonal matrix elements might, in principle, also vary in response to displacements of neighboring atoms and orbital reorthogonalization. The change in diagonal matrix elements is given as a function of off-diagonal matrix elements:

$$E_{\vec{R}\alpha} = E^0_{\vec{R}\alpha} + \sum_{\vec{R}\in nn}\sum_{\beta} C_{\vec{R}\alpha,\vec{R}'\beta}\frac{t^0_{\vec{R}\alpha,\vec{R}'\beta} - t'_{\vec{R}\alpha,\vec{R}'\beta}}{E^0_{\vec{R}\alpha} + E^0_{\vec{R}'\beta}}, \quad (3)$$

where C are empirical material parameters determined by fitting to bulk properties. This model has a form suitable for atomistic calculation as all quantities are expressed in terms of matrix elements related (via Slater-Koster rules and Harrsion law) to bond angles and lengths. Aiming to be more general than the work by Jancu *et al.*,[41] the Boykin model[43] takes into account strain-related changes of all diagonal matrix elements, however at a cost of introducing 16 new empirical constants per material apart from 14 power-law exponents. Unambiguous fit for such a large number (30) of empirical parameters is, in my opinion, difficult, if not impossible.

Recently Niquet *et al.*[45] and Boykin *et al.*[46] introduced models with same site (on-site), off-diagonal matrix elements for accurate modeling of uniaxial [111] and [110] strains. Authors of these papers argue that on-site matrix elements changes arise both from changes in Löwdin orbitals and nearest-neighbors potential. These parametrizations introduce an additional 13 or 16 empirical parameters (correspondingly in Niquet *et al.*[45] and Boykin *et al.*[46] cases), resulting in a cumbersome fitting process. Additionally same site, off-diagonal tight-binding approaches need special attention in order to avoid breaking of gauge invariance.[46,48,49] In the next section of this paper I adopt the Jancu *et al.* model and reexpress formula (2) in language suitable for atomistic calculation.

III. COUPLING STRAIN INTO ATOMISTIC HAMILTONIANS

Let us start by observing that the diagonal part of the strain tensor can be decomposed into purely hydrostatic and purely

biaxial (volume conserving or "traceless") strains:

$$\begin{pmatrix} \epsilon_{xx} & 0 & 0 \\ 0 & \epsilon_{yy} & 0 \\ 0 & 0 & \epsilon_{zz} \end{pmatrix} = \frac{1}{3}\begin{pmatrix} Tr(\epsilon) & 0 & 0 \\ 0 & Tr(\epsilon) & 0 \\ 0 & 0 & Tr(\epsilon) \end{pmatrix} + \frac{2}{3}\begin{pmatrix} \epsilon_{xx} - \frac{(\epsilon_{yy}+\epsilon_{zz})}{2} & 0 & 0 \\ 0 & \epsilon_{yy} - \frac{(\epsilon_{xx}+\epsilon_{zz})}{2} & 0 \\ 0 & 0 & \epsilon_{zz} - \frac{(\epsilon_{xx}+\epsilon_{yy})}{2} \end{pmatrix} \quad (4)$$

where $Tr(\epsilon) = \epsilon_{xx} + \epsilon_{yy} + \epsilon_{zz}$.

From the linear deformation potential theory one expects changes of the Hamiltonian matrix elements to be proportional to the deformation, with the proportionality factor being the deformation potential. For the pure hydrostatic strain $\epsilon_{xx} = \epsilon_{yy} = \epsilon_{zz}$ the biaxial part vanishes and the hydrostatic strain would lead to mere shifts of level energies, without altering system symmetry. The biaxial part of formula four on the other hand can reduce system symmetry and split degenerate levels. However being traceless it does not change (in linear regime) the average energy of split multiplets.

In the empirical pseudopotential method $Tr(\epsilon)$ explicitly enters the local part[29,30] of the pseudopotential to include dependence on the local hydrostatic strain that should be accounted for in a non-self-consistent calculation to reproduce correctly the target deformation potential of the valence band.[29,30] In the tight-binding picture the hydrostatic deformation is typically accounted for not through linear modification of diagonal matrix elements, but by introducing changes of hopping matrix elements governed by Harrison law, going thus beyond the linear limits of formula (4). Similarly, axial strains are accounted for by Slater-Koster angular rules in off-diagonal terms, therefore including (apart from uniaxial [001] strains) also shear strains (strain tensor off-diagonals related to [111] uniaxial strain), again going beyond the limits of formula (4).

To summarize, in the tight-binding formalism the off-diagonal matrix elements account for both the volume and the angular strain effects. However, it turns out[41–43,45,46] that in order to achieve a satisfactory description (fits) of experimental deformation potentials, splitting due to uniaxial strain of diagonal terms (d orbitals energies) needs to be accounted for explicitly in the TB Hamiltonian. The degree to which such diagonal parameter modifications are needed appears to be model dependent,[43] however the physical background for such approaches has been recently[46] given a solid justification in terms of contributions due to displacement of the nearest-neighbor potentials and orbital (Löwdin) renormalization effects.

Should one use continuum elasticity approach[21] for the calculation of strained fields, one could calculate[17] the local strain tensor at each site of the rectangular computational (finite differences) grid. However in this work I use an atomistic (valence force field[50,51]) approach for the calculation of strained atomic positions, with atoms occupying sites of a complicated (lower-symmetry) crystal lattice. While Eq. (2) is directly applicable to a simple cubic lattice, for a more complicated zinc-blende (or wurtzite) tetragonally oriented crystal a different approach is needed. To overcome this technical difficulty Pryor and co-workers[21] have introduced a method for calculation of local (microscopic) strain tensor by comparison of the strained and the unstrained tetrahedron spanned by atom and its nearest neighbors, where the strain tensor ϵ at a given (atomic) site can be calculated as[21]

$$\begin{pmatrix} \epsilon_{xx} & \epsilon_{yx} & \epsilon_{zx} \\ \epsilon_{xy} & \epsilon_{yy} & \epsilon_{zy} \\ \epsilon_{xz} & \epsilon_{yz} & \epsilon_{zz} \end{pmatrix} = \begin{pmatrix} R_{12,x} & R_{23,x} & R_{34,x} \\ R_{12,y} & R_{23,y} & R_{34,y} \\ R_{12,z} & R_{23,z} & R_{34,z} \end{pmatrix} * \begin{pmatrix} R^0_{12,x} & R^0_{23,x} & R^0_{34,x} \\ R^0_{12,y} & R^0_{23,y} & R^0_{34,y} \\ R^0_{12,z} & R^0_{23,z} & R^0_{34,z} \end{pmatrix}^{-1} - I, \quad (5)$$

where $R_{ij,k}$ describes the k component of the R_{ij} vector connecting neighboring atoms i and j for the distorted (strained) tetrahedron, while $R^0_{ij,k}$ corresponds to the ideal (bulk equilibrium) case. I is an identity matrix.

Equation (5) has been derived[21] by comparison of the distorted tetrahedron formed by the four nearest neighbors of the atom at R and the ideal tetrahedron in the unstrained bulk. The local strain tensor is thus calculated at a cation site (for cation-mixed systems, e.g., InAs/GaAs) by considering a tetrahedron formed by four nearest neighboring anions or at an anion site (for anion-mixed systems, e.g., InAs/InP) by considering a tetrahedron formed by four nearest neighboring cations. The drawback of the above formulation is that it is not well defined for interface atoms that have neighbors of different atomic species (anions for cation mixed systems or cations for anion mixed system), as it is not univocal how to define the ideal, unstrained tetrahedron in such a case. This "ambiguity" has been noticed in the empirical pseudopotential method,[29,30] where the hydrostatic strain correction to the local part of the pseudopotential is set to zero for interface As atoms "to avoid any ambiguity due to shared As atoms at InAs/GaAs interfaces".[30] More importantly, Eq. (5) defines strain tensor only for one of the ionic species (cations for InAs/GaAs and anions for InAs/InP systems), while the strain tensor remains undefined for the other (common/shared) ionic species. In principle one could adopt an interpolation approach and calculate ϵ at a common ion (including interface atoms) as an average of ϵ's derived at surrounding atoms. In this work I use a bit different approach that also removes the necessity of explicitly building R and R^0 matrices. First I utilize the fact that one can express vector $R_{ij,k}$ in terms of direction cosines n_i, l_i, m_i and bond length d_i between an atom and its neighbors, e.g.: $R_{12,x} = d_2 n_2 - d_1 n_1$, then by substituting this relation into Eq. (5) I can express strain tensor elements in terms of bond length and angles.[52] For example biaxial strain along the [001] direction would be given as

$$B_{xy} = \epsilon_{zz} - \frac{(\epsilon_{xx} + \epsilon_{yy})}{2} = \sum_i^N \left(d_i/d_i^0\right)\left[\frac{m_i}{m_i^0} - \frac{1}{2}\left(\frac{n_i}{n_i^0} + \frac{l_i}{l_i^0}\right)\right], \quad (6)$$

where the summation goes over N nearest neighbors, n_i,l_i,m_i are direction cosines corresponding to neighbor number i, and n_i^0,l_i^0,m_i^0 are direction cosines for the bulk equilibrium case. Biaxial strain is thus given in terms of contributions from (four) bonds of neighboring atoms.

Substituting this expression into Eq. (2) I obtain an expression[52] for a shift of diagonal matrix elements corresponding to the d_{xy} orbital:

$$E_{xy} = E_d + \frac{2b_d}{N}\sum_i^N \left(d_i/d_i^0\right)\left[\frac{m_i}{m_i^0} - \frac{1}{2}\left(\frac{n_i}{n_i^0} + \frac{l_i}{l_i^0}\right)\right], \quad (7)$$

and similar formulas for E_{yx} and E_{zx} orbitals.

Due to its formal and numerical simplicity formula (7) is one of the most important results of this work and has several advantages: It is expressed in terms of bond lengths and angles only, therefore suitable for nanosystem calculation, while (for bulk) it gives the same strained band edges evolution as that given by Eq. (2). It uses only one empirical parameter per one bulk material. It is much less computationally demanding then analogous Eq. (3) by Boykin and co-workers. It can also be generalized for interface atoms that have two sorts of neighboring species (e.g., interface *As* that have both In and Ga as neighbors), for which is it not unequivocal how to calculate strain tensor in the continuous matter approximation. While the problem of the accurate interface atoms treatment is still present in this approach, I propose b_d to be taken as average over all neighbors, however more elaborate schemes (e.g., *ab initio* derived b_d) could be, in principle, considered. Finally, formulas similar to Eq. (7) can be obtained for more general models including trigonal deformations, aiming to account for strain along [111] (Ref. 42), which will be the subject of my future work.

IV. APPLICATION

I illustrate my method with the example of a lens-shaped self-assembled InAs embedded in either a InP or GaAs matrix. In order to compare with the EPM calculations[28,29,31,32] the height of the lens-shaped dot is chosen as $h = 3.5$ nm and the base diameter is $D = 25$ nm.

There is a lattice mismatch between dot material (InAs) and surrounding matrix material (InP/GaAs). To calculate strain relaxed positions I use the atomistic valence force field (VFF) approach of Keating.[50] This method is described in more detail in Refs. 21 and 51 and in our previous works.[36,38] The size of computational domain, including more than 50 million atoms, guarantees convergence of the strain distribution.

Single particle states are obtained using these strain relaxed positions, by building the $sp^3d^5s^*$ tight-binding Hamiltonian and then diagonalizing the Hamiltonian by means of the Arnoldi algorithm with the matrix-vector multiplication parallelized using *OpenMP* approach on 48 core, shared memory system. As the number of atoms in the TB domain is larger than half a million, in order to make the entire calculation feasible I calculate only eigenenergies and eigenstates corresponding to several lowest electron and hole confined states.

Due to a small lattice mismatch of InAs and InP I neglect the piezoelectric effects in the present calculation, following similar arguments by Gong *et al.*[31] who ignore piezoelectricity in the empirical pseudopotential work on InAs/InP dots. Consistently, piezoelectric effects can also be neglected for lens-shaped InAs/GaAs dots, where contribution due to second-order effects tends to cancel linear terms.[53] Finally the piezoelectricity is neglected for the sake of comparison with other approaches where this effect is neglected (comment 41 from Ref. 28).

A. The effect of diagonal correction

In order to study the importance of the diagonal correction terms first I have calculated the effective single particle gap, defined as the difference of the electron and the hole ground state energies with the diagonal correction included and neglected [b_d set to zero in Eq. (2) or Eq. (7)]. For InAs/InP quantum dot I have obtained 766.05 meV and 696.52 meV with the diagonal correction included and neglected, while for InAs/GaAs lens-shaped dots I obtained 889.7 meV and 732.08 meV with the diagonal correction included and neglected. Therefore, should the diagonal correction shift be neglected the ETB would predict the single particle gap by ≈60 meV smaller for less strained InAs/InP system and by almost 160 meV smaller for highly strained InAs/GaAs quantum dot.

Single particle gap is the dominant contribution (≈800–1000 meV) to the excitonic gap observed in experiment, with the correction due to electron-hole interaction (≈20 meV) and correlation effects (≈1 meV) being significantly smaller. Robust calculation of this quantity is thus of great importance, especially for reliable comparison with experiment. Such large differences, both relative and absolute, show that the diagonal correction cannot be neglected for strained nanosystem calculation, for tight-binding models requiring diagonal parameter shifts.[41–43]

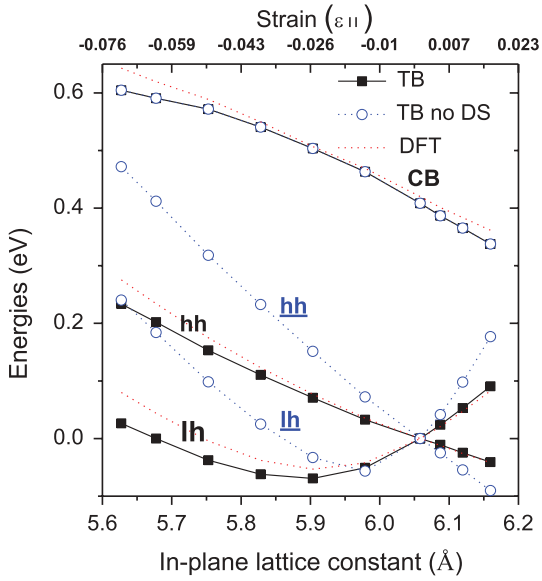

FIG. 1. (Color online) InAs bulk band edges (conduction band, heavy- and light-hole) under biaxial [001] strain as calculated by Jancu *et al.* (Ref. 41) tight-binding model with diagonal shift included (solid lines/full boxes) or artificially neglected (dotted lines/empty boxes). Recent DFT results (Ref. 55) are shown for comparison (dotted/red lines with no symbols).

The origin of this effect can be very well seen on Figure 1 where I show the evolution of bulk (at the Γ-point) conduction, heavy- and light-hole bands as a function [001] biaxial strain.[54] With the diagonal correction included, the bulk bands evolution is in good agreement with recent DFT calculation,[55] especially within small strain range. This agreement is no longer true when the diagonal correction is neglected. The conduction band is built form s states and not thus affected by the diagonal correction. However both hole bands, with the diagonal correction neglected, reveal very strong upward shift and hence strong, erroneous (with respect to bulk target values) reduction of bulk band gap ($CB - HH$). Similar consequences are be observed for quantum dot effective gap and also other spectral quantities. To summarize for TB models requiring diagonal parameter adjustment this correction can be neglected neither for bulk nor nanosystems. While these effects for bulk systems has been already studied in more detail,[41,43] in this paper we focus on more quantitative comparison for quantum dot systems using different approaches and parametrizations.

B. Charge distributions and level spacings

Figure 2 shows charge distributions and energies corresponding to several lowest electron and hole levels calculated for the (a) InAs/InP and (b) InAs/GaAs lens-shaped quantum dots. Shell-like structure of confined electron states is very similar in both cases (InP and GaAs matrix) despite much larger hydrostatic strain in InAs/GaAs quantum dot, with s-p levels ($e_2 - e_1$) spacing on the order of 50 meV and p-shell ($e_3 - e_2$) splitting of ≈2–3 meV.

Interestingly, for a less strained InAs/InP system, the structure of confined hole states is also quite well described by the 2D harmonic oscillator model,[1] with a well pronounced shell structure visible in the energy spectra. In this case the charge densities correspond to clearly defined s-, p-, and d-like states, with orientation of the p hole states being only reversed with respect to electron p states, in agreement with recent empirical pseudopotential calculation.[31]

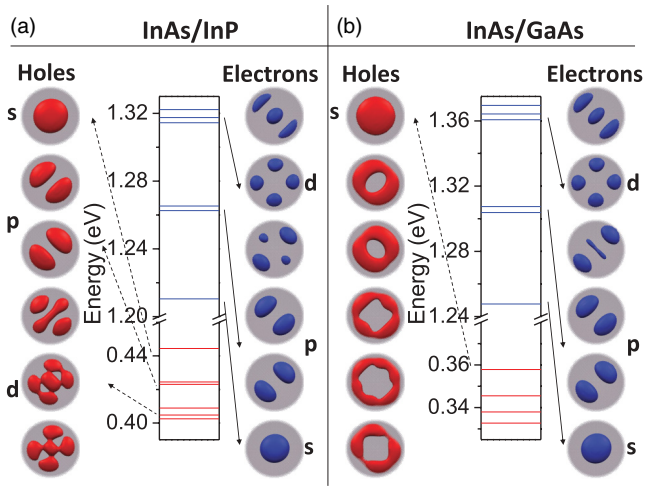

FIG. 2. (Color online) Single particle electron and hole energies and probability density isosurfaces for (a) InAs/InP and (b) InAs/GaAs lens-shaped ($d = 25$ nm, $h = 3.5$ nm) quantum dot.

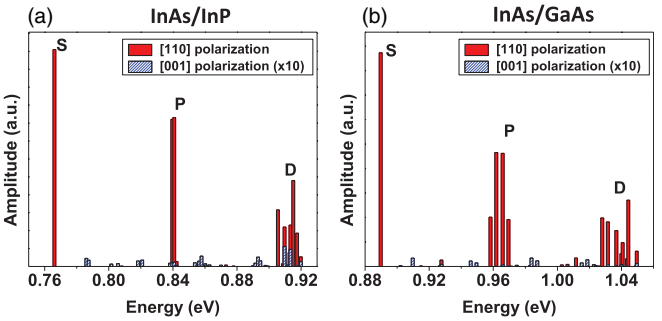

FIG. 3. (Color online) Joint optical density of states (single particle absorption spectra) calculated for light polarized along x (red/light gray/plain) and z (blue/dark gray/patterned) axes for (a) InAs/InP and (b) InAs/GaAs lens-shaped ($d = 25$ nm, $h = 3.5$ nm) quantum dot.

The above shell-like structure is however not present for confined hole states in highly strained InAs/GaAs quantum dots. While the ground hole state in the InAs/GaAs system is of s-like character there are strong splittings of the higher lying levels that have been also noticed in calculations using different approaches[28,29,56] leading to peculiar hole charging patterns observed in experiment.[16]

Figure 3 shows the joint optical density of states[38] (the single-particle absorption spectrum) calculated for (a) InAs/InP and (b) InAs/GaAs lens-shaped quantum dots, for light polarized along [110] and [001] crystal directions (corresponding to quantum dot lateral and growth directions). Due to the dominant confinement in the growth direction, contribution from light polarized along the [001] axis is almost negligible.[38] Well defined, shell-like structure of confined InAs/InP quantum dot levels is visible in Fig. 3(a) with two almost overlapping P lines of similar height, corresponding to single particle transition between electron and hole levels of the same symmetry. For InAs/GaAs quantum dot there are however four separate P lines with different oscillator strengths and ≈10 meV energetic separation due to hole and electron p-shell splittings. The higher energy ("d"-shell) structure is even more complex.

Gong *et al.*[31] speculate that the difference between lens-shaped InAs/InP and InAs/GaAs may be due to valence band offset (VBO) difference between both cases. However in my calculations I used similar band offset for both matrices ($VBO = 0.460$ eV for InAs/InP quantum dot and $VBO = 0.3$ eV InAs/GaAs quantum dot[57–59]), and I suspect it is not the VBO, but rather strain effects that contribute to this difference. More detailed discussion will be given in my future work.

C. Quantitative comparison

Table I shows the single particle level spacings of the InAs/InP and InAs/GaAs dots calculated using my ETB approach compared with the ETB obtained without the diagonal correction shift (b_d set to zero) shown in brackets. As mentioned earlier the inclusion of the diagonal adjustment leads to single particle gap difference reaching up to ≈160 meV for the InAs/GaAs quantum dot, which constitutes about 20% of the quantum dot single particle gap value. However, other electron and hole level spacings are also influenced

TABLE I. Comparison of this work empirical tight-binding (ETB1), empirical tight-binding (ETB2) approach from Ref. 43, and the empirical pseudopotential (EPM1—Ref. 28, EPM2—Ref. 29, EPM3—Ref. 31) -calculated single-particle level spacings (in meV) of the InAs/GaAs and InAs/InP lens-shaped ($d = 25$ nm, $h = 3.5$ nm) quantum dot. Tight-binding results obtained without diagonal correction shift (b_d or $C_{\vec{R}\alpha,\vec{R}'\beta}$ set to zero) are shown for comparison in brackets. Additionally I compare InAs gap hydrostatic deformation potentials (a_g^{InAs} in eV) reproduced in different approaches and the electron-hole Coulomb energy $J_{e_1h_1}$ of the ground electron-hole s states (in meV).

	InAs/GaAs				InAs/InP	
	ETB1	ETB2	EPM1	EPM2	ETB1	EPM3
$e_2 - e_1$ (s-p)	56.15 (59.91)	47.16 (53.05)	57.0	65	52.16 (53.9)	53.6
$e_3 - e_2$ (p shell)	3.6 (4.29)	2.48 (1.80)	2.1	2	2.65 (2.92)	2.2
$e_4 - e_3$ (p-d)	53.33 (55.16)	46.28 (52.27)	58.7	68	49.17 (49.94)	48.0
$h_2 - h_1$ (s-p)	12.35 (14.51)	9.08 (0.01)	11.3	8	19.95 (21.75)	25.2
$h_3 - h_2$ (p shell)	7.59 (9.81)	7.27 (4.54)	9.5	7	1.45 (2.32)	1.2
$h_4 - h_3$ (p-d)	5.2 (5.31)	3.64 (0.33)	2.4	6	14.09 (15.83)	17.6
$e_1 - h_1$ (s-p)	889.7 (732.08)	826.67 (797.43)	1017.5	1062	766.05 (696.52)	828.70
a_g^{InAs} (eV)	−6.08	−6.08	−6.78	−6.79	−6.08	−6.44
$J_{e_1h_1}$	22.22	21.5	21.8	30	22.56	20.3

by inclusion of the diagonal adjustment. Importantly, while the absolute differences are of the order of several meV, the relative differences are noticeable, especially for hole p-shell splittings. Interestingly, despite the fact that diagonal correction (at the Γ-point) influences bulk valence[41] states only (as seen before in Fig. 1), in a confined quantum dot system, due to band- and valley-mixing effects, the electron state energies are also affected by the inclusion of diagonal adjustments. The difference is especially large for electron p-shell splitting.

In order to study the role of the diagonal correction I have additionally implemented a model by Boykin and co-workers[43,44] and a performed calculation for the InAs/GaAs system for which the parameters are given in literature.[44] Results of this calculation are again shown in Table I, denoted as ETB2 with the diagonal correction shift included and diagonal shift neglected values shown in brackets [$C_{\vec{R}\alpha,\vec{R}'\beta}$ constants in Eq. (3) set to zero]. With the diagonal terms included I find reasonable agreement between both ETB approaches, with similar shell-like structure for electron and holes, and the small differences between two methods can probably be explained in terms of different fitting approaches or fitting targets (most importantly GaAs bulk band gap) used in these parametrizations.

Interestingly, in a recent work of Díaz and Bryant,[35] different ETB parametrizations (including Jancu *et al.*[41] and Boykin *et al.*[43]) were applied to (strain-free) GaAs nanocrystals, and indeed the conclusion was that "the parametrization itself, rather than the basis, seems to be responsible for the differences observed." Thus the actual fitting scheme details (e.g., weights in the fitting procedure), which are typically not published, may be more important then the particular ETB model (e.g., $sp^3d^5s^*$) or fitting targets (e.g., gap values).

Importantly, with the diagonal terms neglected in Boykin *et al.*[43] (ETB2) scheme, the single particle gap changes only by ≈30 meV, yet the actual structure of confined states, especially holes states, is dramatically changed, with the ground hole states being nearly doubly degenerate (≈0.01 meV). Such importance of diagonal terms in ETB2 approach can be traced back to the fact that in this approach the valence band offset between InAs and GaAs is embedded in (built into) the diagonal correction and neglecting the diagonal correction results in strongly reduced binding potential for holes, leading to this peculiar hole levels structure.

Table I shows thus that for TB models requiring diagonal parameter adjustment this correction cannot be neglected for nanosystems as it could not be neglected for bulk (as seen in Fig. 1). Table I also shows that accurate modeling of strain effects plays an important role, even for low-strained InAs/InP systems, should the meV accuracy be needed, and that spectral features at different energy range (e.g., effective gap, s-p shell spacing, p shell splitting) can be calculated with different accuracy depending on a given empirical method and a particular parametrization.

Table I shows also the single particle level spacings of the InAs/InP and InAs/GaAs lens type quantum dots calculated using my ETB approach and compared with EPM results. For the InAs/GaAs system I compare the ETB results with two EPM result sets (EPM1—Ref. 28, EPM2—Ref. 29) obtained using the same pseudopotentials[29] (A. Zunger and co-workers), yet interestingly differing most likely due to some other details of the calculation. The EPM results for InAs/InP lens type quantum dot (EPM3) were taken from the recent paper by Gong and co-workers.[31]

There is not only good qualitative, but also quite good quantitative agreement between ETB and the more recent EPM approaches, especially for electron level spacings for the InAs/InP quantum dot. Similarly there is reasonable agreement of electron states spacings calculated for the InAs/GaAs quantum dot, with a more pronounced difference for the electron p-shell splitting. The differences between hole states of InAs/InP quantum dot are larger than that for electrons, yet the overall spectral structure is similar for the two approaches. As mentioned before there is a characteristic shell-like structure: s-p spacing is on the order of 20–25 meV and hole p-shell splitting is ≈1.2–1.4 meV. The difference for the highly strained InAs/GaAs quantum dot is larger, yet the characteristic large hole p-shell splitting dominating over p-d level spacing is reproduced in both approaches as it also was in the Boykin *et al.*[43] (ETB2) tight-binding model.

I believe this is very good agreement taking into account the fact that both methods (ETB1 and EPM1) reproduce bulk effective gaps, masses, and band deformation potentials with certain errors and that both approaches use a slightly different flavor of VFF strain calculation, computational domain sizes, and boundary conditions etc. Interestingly the differences between the recent EPM1 and the older EPM2 empirical pseudopotential calculations are larger then between both ETB approaches and EPM1.

Despite similarities there is a large quantitative difference between the ETB1 and the EPM1 that lies in the most important energy range, i.e., the single particle effective gap. This value is systematically larger for the EPM1 compared to the ETB1, by about 60 meV for the InAs/InP quantum dot and by almost 130 meV for the highly strained InAs/GaAs system.

I think this effect is partially due to the fact that there is a difference (fitting error) between target and fitted absolute gap deformation potential in the empirical pseudopotential approach (e.g., Table I from Ref. 29), with the error bar reaching 0.7–1 eV, i.e., almost 10–15% of the fitting target (−6.0 eV).[29,31] Such errors may lead to overestimation of the single particle gap by ≈60 meV for the highly strained InAs/GaAs system. I do not suggest however that the EPM is less accurate than the ETB, and it is not the author's intention to undermine the importance or accuracy of any method, but just to emphasize the role of (difficult and tedious) fitting processes in any empirical calculation. It should be noted that authors of the original EPM1 paper acknowledge the problem (p. 12 964 from Ref. 29): "The main approximations involved in our method are a) the fit of the pseudopotential to the experimental data for bulk materials is never perfect [...]." And it is fair to assume that similar limits apply also to the ETB or any empirical approach. It should be also noted that in fact most of the fitting targets in ETB1 and EPM1 approaches are actually quite similar, while these are the achieved fits that differ. Thus, even if in both approaches one would use exactly the same fitting targets, the actually reproduced values could in principle be different.

There are in fact two important fitting targets that differ between the EPM and the ETB approaches and could lead to some of the observed differences. These are different values of unstrained valence band offset VBO and the different sign of the absolute hole deformation potential a_v in both approaches. The EPM uses $a_v = -1.0$ eV while my approach (and Jancu *et al.*[41] parametrization) gives positive $a_v = 1.0$ eV value in agreement with recent *ab initio* calculation.[59] Similarly the EPM systematically uses very small 50–60 meV valence band offset (for InAs/GaAs systems) in contrast with the ETB 200–300 meV values,[57] being again in good agreement with recent *ab initio* studies.[57,59] However, it should be pointed out that while "natural," i.e., strain free, VBO and a_v differ significantly between two methods, it is the strained band offset (being a "combination" of both) that enters the calculation as the actual hole confining potential.[55] And more importantly this strained band offset obtained by using two sets of a_v and VBO parameters is very similar, ≈330 meV. Thus, in result, the effective confining potentials in the ETB and the EPM approaches are quite similar despite noticeably different bulk ("intermediate") target values. As this needs a further study I will discuss the role of these differences in more detail in future work.

Next, in Table I, I compare electron-hole Coulomb (direct) energy $J_{e_1h_1}$ calculated[23,38] for the electron and the hole occupying their ground s states. The numbers are again comparable, despite different models of incorporating[38] screening effects in both approaches, resulting in larger screening (smaller integrals) in empirical pseudopotential approach. Again, interestingly, there is a larger difference between different empirical pseudopotential approaches than between the ETB1/ETB2 and the EPM1. Detailed comparison of ETB/EPM many-body effects goes beyond the scope of this work, yet I notice that despite the discussed difference of single particle gaps predictions, the exciton binding energy (well approximated by $J_{e_1h_1}$) is comparable in all approaches, a manifestation of long-range character of Coulomb direct interactions. I conclude that in empirical calculations spectral features at different energy scales can be calculated with different accuracy, depending on a given empirical method and a particular parametrization.

D. Role of valence force field parameterization

Finally, I study the effect of different valence force field parametrizations on the single particle spectra of confined quantum dot states. There are two empirical force constants (α,β) used in Keating's VFF approach[50] that are fit to reproduce bulk elastic properties (namely c_{11},c_{12}, and c_{44} bulk elastic constants). At least two fitting schemes and thus two VFF parametrization schemes are possible. In a more traditional[50,60] approach, two α, β parameters are obtained directly from the bulk elastic c_{11} and c_{12} constants only, while c_{44} constant is not a fitting target, but rather comes as an output of the "fitting" process, sometimes resulting in a substantial error of c_{44} as seen in Table II (parameterization VFF1). Such an approach can be however well justified for [001] growth where strain properties are dominated by hydrostatic and biaxial component related to c_{11} and c_{12}, and these constants should be well reproduced (VFF1 parametrization Table II), while shear (off-diagonal) strains related to c_{44} are negligible. The latter is unfortunately not always true especially for [111] growth. To overcome this difficulty, recently a scheme which fits VFF parameters to all three bulk constants on similar footing has been proposed.[61] This fit is performed to reproduce bulk modulus $K = (c_{11} + 2c_{12})/3$ and c_{44} explicitly (parameterization VFF2 in Table II).

I used both of these parametrizations to calculate strained positions that were later used as input into the ETB single

TABLE II. Comparison of bulk elastic constants c_{11}, c_{12}, and c_{44} (in GPa) reproduced by different valence force field parametrizations [VFF1 (Ref. 21) and VFF2 (Ref. 61)] and obtained from experiment (Ref. 62).

	$c_{11}(GPa)$	$c_{12}(GPa)$	$c_{44}(GPa)$
VFF1	85.30	49.00	31.40
VFF2	90.27	41.77	39.59
Exp.	83.29	45.26	39.59

TABLE III. Comparison of the empirical tight-binding-calculated single-particle level spacings (in meV) and electron-hole Coulomb energy $J_{e_1h_1}$ of the ground electron-hole s states of the InAs/InP and InAs/GaAs lens-shaped ($d = 25$ nm, $h = 3.5$ nm) quantum dot reproduced by different valence force field parametrizations [VFF1 (Ref. 21) and VFF2 (Ref. 61)].

	InAs/GaAs		InAs/InP	
	VFF1	VFF2	VFF1	VFF2
$e_2 - e_1$ (s-p)	56.15	51.10	52.16	49.85
$e_3 - e_2$ (p shell)	3.6	3.4	2.65	2.55
$e_4 - e_3$ (p-d)	53.33	48.47	49.17	47.06
$h_2 - h_1$ (s-p)	12.35	13.89	19.95	19.91
$h_3 - h_2$ (p shell)	7.59	5.47	1.45	1.52
$h_4 - h_3$ (p-d)	5.2	8.32	14.09	13.61
$e_1 - h_1$ (s-p)	889.7	1000.1	766.05	810.53
$J_{e_1h_1}$	22.22	22.71	22.55	22.72

particle spectra calculation, and compared results in Table III. While the electron-hole Coulomb direct energy is generally unaffected by the choice of VFF parameters, the differences between VFF parametrizations, especially for the description of the single particle gap, are comparable to the large differences between two entirely different approaches (ETB and EPM). There is ≈110 meV larger gap for the InAs/GaAs system described by the VFF2 parameters compared to the VFF1 case.

The VFF2 was developed[61] to reproduce c_{44} and thus Poisson ratio $v_{111} = 2\frac{c_{11}+2c_{12}-2c_{44}}{c_{11}+2c_{12}+4c_{44}}$ for strain along the [111] direction;[61,63] it is thus preferred for modeling of systems grown along the [111] axis. However, for [001] strain the VFF2 reproduces the Poisson ratio $v_{001} = \frac{2c_{12}}{c_{11}}$ with ≈15% error. I speculate that due to this, the VFF2 will generally overestimate single particle gap for [001] growth and underestimate (due to shallower confinement) electron single particle s-p and p-d level spacings. As expected for larger strain, the differences between two VFF parametrizations will be more pronounced, and thus spacings of the single particle hole levels for highly strained InAs/GaAs quantum dot differ noticeably between the two (VFF1 and VFF2) cases.

I find the VFF2 parametrization not fully suitable for description of [001] grown quantum dots. On the other hand, it reproduces very well the c_{44} constant (Table III) and is thus more appropriate for description of [111] growth. I believe that further research is needed on the subject and conclude that caution should be exercised before applying different VFF models and parametrizations.

V. SUMMARY

I have demonstrated a method of coupling strain into tight-binding models suitable for calculation of electronic and optical properties of semiconductor nanosystems. I have obtained a simple diagonal correction formula using only one empirical, on-site parameter per bulk material and have applied this method to lens-shaped InAs/InP and InAs/GaAs quantum dots. I found that there are noticeable differences between both systems, especially for confined hole states that need to be further analyzed. I have shown that for TB models requiring diagonal parameter adjustment this correction can be neglected neither for bulk nor nanosystems. I have obtained comparable results (both qualitatively and quantitatively) from well-established empirical pseudopotential methods and an alternative empirical tight-binding approach. I have found that in empirical calculations spectral features at different energy scales can be calculated with different accuracy, depending on the empirical method and a particular parametrization.

ACKNOWLEDGMENTS

This work was supported by the Foundation for Polish Science, Homing Plus Programme co-financed by the European Union within the European Regional Development Fund. The author would like to thank G. W. Bryant, W. Jaskólski, P. Rożański, and J. Zielińska for careful reading of the manuscript.

*mzielin@fizyka.umk.pl

[1] L. Jacak, P. Hawrylak, and A. Wojs, *Quantum Dots* (Springer, Berlin, 1998).
[2] D. Bimberg, M. Grundmann, and N. N. Ledentsov, *Quantum Dot Heterostructures* (Wiley, New York, 1998).
[3] C. Delerue and M. Lannoo, *Nanostrucutres: Theory and Modelling* (Springer, Nanosciences and Technology Series, 2004).
[4] *Nanocrystal Quantum Dots*, edited by Victor I. Klimov (CRC Press, New York, 2012).
[5] D. Chithrani, R. L. Williams, J. Lefebvre, P. J. Poole, and G. C. Aers, Appl. Phys. Lett. **84**, 978 (2004).
[6] E. D. Minot, F. Kelkensberg, M. van Kouwen, J. A. van Dam, L. P. Kouwenhoven, V. Zwiller, M. T. Borgstrm, O. Wunnicke, M. A. Verheijen, and E. P. A. M. Bakkers, Nano Lett. **7**, 367 (2007).
[7] D. Dalacu, K. Mnaymneh, X. Wu, J. Lapointe, G. C. Aers, P. J. Poole, and R. L. Williams, Appl. Phys. Lett. **98**, 251101 (2011).
[8] R. Singh and G. Bester, Phys. Rev. Lett. **103**, 063601 (2009).
[9] R. Singh and G. Bester, Phys. Rev. Lett. **104**, 196803 (2010).
[10] G. W. Bryant, M. Zielinski, Natalia Malkova, J. Sims, W. Jaskolski, and J. Aizpurua, Phys. Rev. Lett. **105**, 067404 (2010).
[11] T. Takagahara, Phys. Rev. B **62**, 16840 (2000).
[12] E. Kadantsev and P. Hawrylak, Phys. Rev. B **81**, 045311 (2010).
[13] S. Tomi and N. Vukmirovi, J. Appl. Phys. **110**, 053710 (2011).
[14] O. Marquardt, S. Schulz, Ch. Freysoldt, S. Boeck, T. Hickel, E. P. OReilly, and J. Neugebauer, Opt. Quantum Electron. **44**, 183 (2012).
[15] K. F. Karlsson, M. A. Dupertuis, D. Y. Oberli, E. Pelucchi, A. Rudra, P. O. Holtz, and E. Kapon, Phys. Rev. B **81**, 161307 (2010).
[16] M. Ediger, G. Bester, A. Badolato, P. M. Petroff, K. Karrai, A. Zunger, and R. J. Warburton, Nat. Phys. **3**, 774 (2007).
[17] G. L. Bir and G. E. Pikus, *Symmetry and Strain-Induced Effects in Semiconductors* (Wiley, New York, 1975).
[18] M. Grundmann, O. Stier, and D. Bimberg, Phys. Rev. B **52**, 11969 (1995).

[19]O. Stier, M. Grundmann, and D. Bimberg, Phys. Rev. B **59**, 5688 (1999).
[20]V. Mlinar and F. M. Peeters, Appl. Phys. Lett. **89**, 261910 (2006).
[21]C. Pryor, J. Kim, L. W. Wang, A. J. Williamson, and A. Zunger, J. Appl. Phys. **83**, 2548 (1998).
[22]G. W. Bryant, M. Zielinski, Natalia Malkova, J. Sims, W. Jaskolski, and J. Aizpurua, Phys. Rev. B **84**, 235412 (2011).
[23]S. Schulz, S. Schumacher, and G. Czycholl, Phys. Rev. B **73**, 245327 (2006).
[24]S. Lee, L. Jönsson, J. W. Wilkins, G. W. Bryant, and G. Klimeck, Phys. Rev. B **63**, 195318 (2001).
[25]K. Leung and K. B. Whaley, Phys. Rev. B **56**, 7455 (1997).
[26]A. Canning, L. W. Wang, A. Williamson, and A. Zunger, J. Comp. Phys. **160**, 29 (2000).
[27]G. Bester and A. Zunger, Phys. Rev. B **71**, 045318 (2005).
[28]L. He and A. Zunger, Phys. Rev. B **73**, 115324 (2006).
[29]A. J. Williamson, L. W. Wang, and A. Zunger, Phys. Rev. B **62**, 12963 (2000).
[30]A. J. Williamson and Alex Zunger, Phys. Rev. B **59**, 15819 (1999).
[31]M. Gong, K. Duan, Ch.-F. Li, R. Magri, G. A. Narvaez, and L. He, Phys. Rev. B **77**, 045326 (2008).
[32]M. Gong M, W. Zhang, G. Can Guo G, and L. He, Appl. Phys. Lett. **99**, 231106 (2011).
[33]J.-W. Luo, A. Franceschetti, and A. Zunger, Phys. Rev. B **78**, 035306 (2008).
[34]R. Santoprete, B. Koiller, R. B. Capaz, P. Kratzer, Q. K. K. Liu, and M. Scheffler, Phys. Rev. B **68**, 235311 (2003).
[35]J. G. Diaz and G. W. Bryant, Phys. Rev. B **73**, 075329 (2006).
[36]W. Jaskólski, M. Zieliński, G. W. Bryant, and J. Aizpurua, Phys. Rev. B **74**, 195339 (2006).
[37]M. Korkusiński, M. Zieliński, and P. Hawrylak, J. Appl. Phys. **105**, 122406 (2009).
[38]M. Zielinski, M. Korkusinski, and P. Hawrylak, Phys. Rev. B **81**, 085301 (2010).
[39]J. C. Slater and G. F. Koster, Phys. Rev. **94**, 1498 (1954).
[40]W. A. Harrison, *Electronic Structure and the Properties of Solids* (Freeman, New York, 1980).
[41]J. M. Jancu, R. Scholz, F. Beltram, and F. Bassani, Phys. Rev. B **57**, 6493 (1998).
[42]J. M. Jancu and P. Voisin, Phys. Rev. B **76**, 115202 (2007).
[43]T. B. Boykin, G. Klimeck, R. C. Bowen, and F. Oyafuso, Phys. Rev. B **66**, 125207 (2002).
[44]G. Klimeck, F. Oyafuso, T. B. Boykin, R. C. Bowen, and P. von Allmen, Computer Modeling in Engineering & Sciences **3**(5), 601 (2002).
[45]Y. M. Niquet, D. Rideau, C. Tavernier, H. Jaouen, and X. Blase, Phys. Rev. B **79**, 245201 (2009).
[46]T. B. Boykin, M. Luisier, M. Salmani-Jelodar, and G. Klimeck, Phys. Rev. B **81**, 125202 (2010).
[47]D. J. Chadi, Phys. Rev. B **16**, 790 (1977).
[48]B. A. Foreman, Phys. Rev. B **66**, 165212 (2002).
[49]T. B. Boykin, R. C. Bowen, and G. Klimeck, Phys. Rev. B **63**, 245314 (2001).
[50]P. N. Keating, Phys. Rev. **145**, 637 (1966); R. M. Martin, Phys. Rev. B **1**, 4005 (1970).
[51]T. Saito and Y. Arakawa, Physica E **15**, 169 (2002).
[52]MATHEMATICA code of these expressions is available on the web page http://fizyka.umk.pl/∼mzielin/codes/CouplingStrainToTB.nb.
[53]G. Bester, A. Zunger, X. Wu, and D. Vanderbilt, Phys. Rev. B **74**, 081305 (2006).
[54]P. R. C. Kent, G. L. W. Hart, and A. Zunger, Appl. Phys. Lett. **81**, 4377 (2002).
[55]E. S. Kadantsev and P. Hawrylak, Appl. Phys. Lett. **98**, 023108 (2011).
[56]A. Schliwa, M. Winkelnkemper, and D. Bimberg, Phys. Rev. B **76**, 205324 (2007).
[57]I. Vurgaftman, J. R. Meyer, and W. L. R. Ram-Mohan, Appl. Phys. Rev. **89**, 5815 (2001).
[58]Chris G. Van de Walle, Phys. Rev. B **39**, 1871 (1989).
[59]Y. H. Li, X. G. Gong, and S. H. Wei, Phys. Rev. B **73**, 245206 (2006).
[60]Y. Cai and M. F. Thorpe, Phys. Rev. B **46**, 15879 (1992).
[61]Y. M. Niquet, Phys. Rev. B **74**, 155304 (2006).
[62]*Physics of Group IV Elements and IIIV Compounds*, edited by O. Madelung, M. Schulz, and H. Weiss, Landolt-Börnstein, New Series, Group III, Vol. 17, Pt. A (Springer-Verlag, New York, 1982).
[63]T. Hammerschmidt, P. Kratzer, and M. Scheffler, Phys. Rev. B **75**, 235328 (2007).